Atmos. Chem. Phys. Discuss., 10, 29809–29851, 2010
www.atmos-chem-phys-discuss.net/10/29809/2010/
doi:10.5194/acpd-10-29809-2010

Atmospheric Chemistry and Physics Discussions

Nonlinear response of ozone to precursor emission changes in China: a modeling study using response surface methodology

J. Xing[1], S. X. Wang[1], C. Jang[2], Y. Zhu[3], and J. M. Hao[1]

[1]Department of Environmental Science and Engineering, and State Key Joint Laboratory of Environment Simulation and Pollution Control, Tsinghua University, Beijing 100084, China
[2]The US Environmental Protection Agency, Research Triangle Park, NC 27711, USA
[3]School of Environmental Science and Engineering, South China University of Technology, Guangzhou 510006, China

Received: 6 September 2010 – Accepted: 24 November 2010 – Published: 7 December 2010

Correspondence to: J. M. Hao (hjm-den@tsinghua.edu.cn)

Published by Copernicus Publications on behalf of the European Geosciences Union.

Abstract

Statistical response surface method (RSM) is successfully applied in Community Multi-scale Air Quality model (CMAQ) analysis on ozone sensitivity studies. Prediction performance has been validated through cross validation, out of sample validation and isopleths validation. Sample methods and key parameters including the maximum numbers for variables involving in statistic interpolation as well as training sample number have been tested and selected through computational experiments. Overall impacts from individual sources including local/regional NO_x and VOC emission sources and NO_x emissions from power plants for three megacities as Beijing, Shanghai and Guangzhou have been evaluated through RSM analysis under a July 2005 modeling study. NO_x control appears to be beneficial for ozone reduction in the downwind areas where usually have higher ozone levels, and it's likely to be more effective than anthropogenic VOC control during heavy photochemical pollution period. Regional NO_x sources are strong contributors to surface ozone mixing. Local NO_x emission control without regional involvement may bring the risk of increasing urban ozone levels due to the VOC-limited conditions, but it gives considerable control benefit for ozone in upper layers (up to 1 km, where the ozone chemistry is changed to NO_x-limited condition) and helps to improve regional air quality in the downwind areas. Effectiveness of NO_x emission control is growing along with stricter control efforts, therefore an integrated regional and multi-pollutant control policy is necessary to mitigate ozone problem in China.

1 Introduction

Tropospheric ozone is not only a key air pollutant that affects human health, crop productivity and natural ecosystems, but also a greenhouse gas that affects global climate. During the past two decades, the rapid economic growth in China has resulted in a significant increase in the emissions of ozone precursors such as nitrogen oxides (NO_x)

ACPD
10, 29809–29851, 2010

and volatile organic compounds (VOC) (Ohara et al., 2007; Wei et al., 2008; Zhang et al., 2009a). The large emissions lead to the formation of elevated ozone over urban and downwind suburban areas. High ozone concentrations over 200 $\mu g\,m^{-3}$ (approximately 103 ppb, the 1-h maximal concentration defined by National Ambient Air Quality Standard of China, Class II) have been frequently observed by in-situ monitoring in east China in recent years (Shao et al., 2006, 2009; Wang et al., 2006a,b,c; Zhang et al., 2008; Tang et al., 2009; Tie et al., 2009; Ran et al., 2009).

Effective attainment of ground-level ozone standards depends upon the reliable estimation of ozone responsiveness to controls of its precursor emissions (Cohan et al., 2006, 2007). In general, ozone formation is classified into two categories of chemical regimes, NO_x-limited and VOC-limited regimes. In the NO_x-limited regime, ozone increases with increasing NO_x and exhibits only slight sensitivity to VOC; in the VOC-limited (or NO_x-rich) regime, ozone increases with increasing VOC and exhibits slight or even negative sensitivity to NO_x. Transitional conditions of dual sensitivity also occur. Classification of ozone production regime helps determine whether NO_x or VOC emissions should be targeted more aggressively in strategies to reduce ozone. However, ozone responsiveness is challenging to simulate due to the spatial/temporal variations of precursor emissions and meteorological conditions (Seinfeld and Pandis, 2006).

Indicators such as NO_y, H_2O_2/HNO_3 and $H_2O_2/(O_3+NO_2)$ simulated by air quality model are used to define the ozone chemistry in a number of studies (Sillman et al., 1995; Tonnesen et al., 2000; Zhang et al., 2009b). Air quality models (AQMs) can be a powerful regulatory tool for comparing the efficacy of various emissions control strategies and policy decisions. Advanced tools embedded in AQMs including ozone source apportionment technology (OSAT) (ENVIRON, 2002; Dunker, et al., 2002; Wang et al., 2009), process analysis (PA) (Jang et al., 1995; Xu et al., 2008; Zhang et al., 2005, 2009; Liu et al., 2010), direct decoupled methods (DDM) and high-order decoupled direct method (HDDM) (Dunker et al., 2002; Hakami et al., 2003; Cohan et al., 2005) enable a better understanding of ozone formation mechanisms. However, due to the often enormous computational costs and the complication of the required emission

ACPD
10, 29809–29851, 2010

inputs and processing, using complex air quality models to generate outputs to meet time-pressing requirements of policy analysis always presents a challenge and is typically inefficient, if not ineffective. A promising tool for addressing this issue, Response Surface Methodology (RSM), has been developed by utilizing advanced statistical techniques to characterize the relationship between model outputs and input parameters in a highly economical manner. The RSM is a metamodel of air quality model. It is a reduced-form prediction model using statistical correlation structures to approximate model functions through the design of complex multi-dimension experiments. The RSM technique has recently been successfully tested and evaluated for a series of $PM_{2.5}$ and ozone assessments and policy analyses in the United States (US EPA, 2006a,b).

In this paper, we develop a response surface model with Community Multi-scale Air Quality (CMAQ) (Byun and Schere, 2006) simulations to investigate ozone sensitivities to NO_x and VOC emission changes in east China during a summer month. The performance of response surface model is validated by additional CMAQ simulations, referred to as out of sample validation, and leave-one-out cross validation. Ozone chemistry in spatial and temporal scale is identified when the precursor emissions change from 0% to 200%. Ozone reduction effectiveness is evaluated when different control measures applied to different sectors in three mega-cities as Beijing, Shanghai and Guangzhou. Synchronized strategies to attain ozone national standards are also discussed.

2 Methodology

The processes involved in developing the ozone RSM application using CMAQ include the selection of modeling domain and configuration, development of multi-dimension experimental design for control strategies, and implementation and validation of the RSM technique, as shown in Fig. 1.

ACPD
10, 29809–29851, 2010

2.1 Emission inventory

Emissions of SO_2, NO_x, PM_{10}, $PM_{2.5}$, BC, OC, NH_3, and NMVOC were calculated based on the framework of the GAINS-Asia model (Amann et al., 2008). The general method used to develop the China regional emission inventory is described in our previous paper (Klimont et al., 2009). To improve the emission estimates, data for emission factors were collected from field measurements performed by Tsinghua University and other published sources in China. A unit-based methodology is applied to estimate emissions from large point sources including coal-fired power plants, iron and steel plants, and cement plants (Zhao et al., 2008; Lei et al., 2008). Detailed local emission information aggregated from the bottom-up investigation of individual power plants, heating boilers, and industries in Beijing (BJ), Yangtze River Delta (YRD) and Pearl River Delta (PRD) are also incorporated into the national emission inventory (Li et al., 2008; Zheng et al., 2009; Wang et al., 2010b). The national emissions in 2005 are summarized in Table 1. The anthropogenic emissions of SO_2, NO_x, PM_{10}, $PM_{2.5}$, BC, OC, NH_3 and NMVOC in China were 28 651 kt, 18 499 kt, 19 237 kt, 14 245 kt, 1595 kt, 3494 kt, 16 556 kt, and 19 406 kt, respectively.

2.2 MM5/CMAQ modeling domain and configuration

The air quality model used to develop response surface model is CMAQ modeling system (ver. 4.7), developed by the US EPA (Byun and Schere, 2006). A one-way nested technique is employed in this study. Modeling domain 1 covers almost entire China with a 36×36 km horizontal grid resolution and generates the boundary conditions for nested subdomain at 12-km resolution over popular Eastern China, as shown in Fig. 2a. The vertical resolution of CMAQ includes fourteen layers from the surface to the tropopause with denser layers at lower altitudes to resolve the planetary boundary layer (PBL). The Carbon Bond Mechanism (CB05) with aqueous and aerosol extensions and the AREO5 aerosol mechanism are chosen for the gas-phase chemistry and aerosol modules, respectively. A spin-up period of six days is used for model

ACPD
10, 29809–29851, 2010

simulations to reduce the influence of initial conditions on model results. The CMAQ simulation period is the entire month of July 2005. A complete description of CMAQ, meteorological, emission, and initial and boundary condition inputs used for this analysis are discussed in Xing et al. (2010) and Wang et al. (2010a). The CMAQ simulations of this modeling system have been validated through comparison with observations of satellite retrievals and surface monitoring data. We compared the simulated ozone concentration with the observed data of six monitoring stations in Beijing, including five urban sites, as Qianmen, Dongsi, Tiantan, Aoti, Nongzhanguan, Gucheng, and one rural site as Dingling, which were described in Streets, et al. (2007) and Wang et al. (2008). The normalized mean bias of simulated hourly ozone concentration during 08:00 a.m.–08:00 p.m. (Beijing time) is 9%, with related coefficient as 0.76. Additionally, the performances of CMAQ simulation on ozone concentration with the same bottom-up emission inventories have been validated by Li et al. (2008) for Yangtze River Delta in January and July 2001, and Wang et al. (2010b) for Beijing in July and August 2008.

2.3 RSM experiment design

RSM uses statistical techniques to build response relationships between a response variable (in this case ozone concentration in this study) and a set of control factors of interest, e.g. emissions of precursor pollutants from particular sources and locations, through designed experiments (Box and Draper, 2007). RSM is a meta-model built upon multi-"Brute Force" model simulations, which can help avoid the uncertainties from the systematical complexity. Due to the limitation of computational capability, design of good experiments is the key issue to build reliable responses with limited samples (Santner et al., 2003), and it is requisite to ensure the accuracy of prediction model. Most of previous studies on O_3 control analyses explored the overall impacts of two factors (total NO_x and total VOC emission) on ozone that may be successfully derived from statistical interpolation of dozens training samples (Milford et al., 1989; Shih et al., 1998; Fu et al., 2006), the interpolation is much more complicated when

ACPD
10, 29809–29851, 2010

the precursor emissions are separated by pollutants, sectors and regions (Wang and Milford, 2001). Constraints are placed on the experimental design space, i.e. the region over which the response is studied, to a set of variables that parameterize a set of possible emissions control strategies, and evaluate the change in ambient ozone levels that result from a change in emissions.

Selection of policy factors was based on precursor emission type and source category relevant to policy analysis of interest. The experimental design carefully considered factors that would provide maximum information for use in comparing relative efficacy of different emissions control strategies. To develop independent response surfaces for particular urban areas, as well as a generalized response surface for all other locations (outside of the particular urban areas), we applied a regional design for the RSM experiment. In this study, the particular urban areas selected are Beijing, Shanghai and Guangzhou. A rigorous area-of-influence analysis was conducted for the selection of RSM urban locations to discern the degree of overlap between different urban areas in terms of air quality impacts, and to tease out local versus regional impacts. The area-of-influence analysis incorporated control model runs where emissions were zeroed out in selected urban areas. Results of these control runs are shown in Fig. 2b. The area-of-influence analysis concluded that ambient ozone concentration in each of the three cities is independent of the precursor emissions from all other areas (the ratios of inner-influence among three regions are less than 3% over the whole vertical height). Thus, selection of these areas allows the RSM to analyze air quality changes in these 3 urban areas independent of one another. On a local or regional basis, the ozone precursor emissions are categorized into NO_x emission from power plants (POW, represents point sources in higher layers), NO_x emission from other area sources (OTH, represents area and mobile sources at the surface layer), and VOC emissions, as shown in Table 2. On the base case emissions shown in Table 1, the emission ratio for each source changes from 0 to 2.

Table 2 gives the sampling method and numbers of training sample used during ozone response surface model development. Method as Hammersley quasi-random

ACPD
10, 29809–29851, 2010

Sequence Sample (HSS) (Hammersley, 1960) which could quickly "fill up" the space in a well-distributed pattern with low discrepancy is adopted in this study. Besides, we choose Latin Hypercube Sample (LHS) (Iman et al., 1980), a widely-used (Wang and Milford, 2001; US EPA, 2006a, b) filling method which ensures that the ensemble of random samples is good representative of the real variability, as an optional choice (Fig. 3a). Based on the uniform-distributed LHS/HSS which has the relative equiprobable interval over the range, additional margin processing is conducted to improve the performance of prediction at margins. Here we choose power function to apply on the samples from uniform-distributed LHS/HSS, as follows:

$$TXn = \begin{cases} X, & n = 1 \\ \left(\frac{X-a}{b-a} \times 2\right)^n \times (b-a) + a, & X \le a + \frac{b-a}{2}, \quad n > 1 \\ \left[1 - \left(\frac{b-X}{b-a} \times 2\right)^n\right] \times (b-a) + a, & X > a + \frac{b-a}{2}, \quad n > 1 \end{cases} \tag{1}$$

Where X is sampled from uniformed LHS/HSS in section $[a, b]$ (in this study we choose [0, 2], which means the emission changes are from all-controlled to be-doubled); TXn is the samples after margin process; n is the order indicting the marginal level.

Another purpose of margin processing is to sample more possible situations. Normally we assume the variables have no direct interaction among each other, however, the variables considered in such predict system are related, e.g., total VOC=VOC from local sources (variable a)+VOC from regional sources (variable b). Samples generated by uniformed methods would provide even distributions for individual source, but non-even for the total emission (here as total VOC) with less samples located in the marginal areas and its density of distribution followed as N (represent the number of pollutant sources) power function, as shown in Fig. 3b. Therefore, margin process is used to enlarge the sample density located in the marginal areas. The optimized marginal level n is selected through computational tests during preliminary experiments (see details in Sect. 3.1.2).

ACPD
10, 29809–29851, 2010

In case LHS1-30, we can simply use 30 training samples generated by LHS method to map the ozone mixing ratios vs. total-NO_x and total-VOC emission ratios. In the case of HSS6-200, 4 types of NO_x emission sources and 2 VOC emission sources are involved, the number of training samples and optimized marginal levels are determined according to the results of preliminary experiments, as shown in Fig. 1 (orange lines). Due to the expensive computational cost of hundreds of CMAQ simulations, we adopt the "quasi-response" of ozone to precursors' emissions based on statistical calculation during preliminary experiments.

The "quasi-response" is based on the results of LHS1-30. Since total emission is the sum of individual emission sources, the emission ratio of total emission is the weight-sum of the emission ratios of each emission source:

$$\mathrm{tNOX} = \sum_{i=1}^{m} \mathrm{NOX}_i, \quad \mathrm{R\text{-}tNOX} = [\mathrm{R\text{-}NOX}_1, \ldots, \mathrm{R\text{-}NOX}_m] \cdot A^{m\times 1} \tag{2}$$

$$\mathrm{tVOC} = \sum_{j=1}^{n} \mathrm{VOC}_j, \quad \mathrm{R\text{-}tVOC} = [\mathrm{R\text{-}VOC}_1, \ldots, \mathrm{R\text{-}VOC}_n] \cdot B^{n\times 1} \tag{3}$$

where tNOX and tVOC are respectively total NO_x emissions and total VOC emissions; NOX_i and VOC_j is emission of each individual source; R-tNOX and R-tVOC are respectively the emission ratio of total NO_x emissions and total-VOC emissions; $\mathrm{R\text{-}NOX}_i$ is the emission ratio of NO_x emission from source i; $\mathrm{R\text{-}VOC}_j$ is the emission ratio of VOC emission from source j; $A^{m\times 1}$ and $B^{n\times 1}$ are the weight coefficients for each NO_x and VOC sources, reflecting contribution from each emission source. One should be noted that such assumption is not always valid, since the long-range transports of regional emissions and large point sources would give different impacts. Such assumption allows us to explore the sensitivity of crucial parameters to the prediction bias through hypothetical computational testing efficiently (see details in Sect. 3.1.2).

ACPD
10, 29809–29851, 2010

2.4 Statistical and prediction method

Each training sample represents one emission control scenario which is simulated by CMAQ and then used for RSM. Based on those simulated ozone responses, RSM prediction system is statistically generalized by MPerK (MATLAB Parametric Empirical Kriging) program followed Maximum Likelihood Estimation – Experimental Best Linear Unbiased Predictors (MLE-EBLUPs) (Santner et al., 2003). The calculation is based the following equation:

$$\boldsymbol{Y}(x_0) = \boldsymbol{Y}_0 = \sum_{j=1}^{d} f_j(x)\boldsymbol{\beta}_j + Z(x) \equiv f_0^T\boldsymbol{\beta} + \boldsymbol{\gamma}_0^T\boldsymbol{R}^{-1}\left(Y^n - F\boldsymbol{\beta}\right) \quad (4)$$

Where $\boldsymbol{Y}(x_0)$ is the predicted concentration from RSM; f_0 is the $d\times1$ vector of regression functions for Y_0^n; F is the $n\times d$ matrix of regression functions for the training data; $\boldsymbol{R}$ is the $n\times n$ matrix of correlations among the Y^n; $\boldsymbol{\gamma}_0$ is the $n\times1$ vector of correlations of Y^n with Y_0^n; $\boldsymbol{\beta}$ is the $d\times1$ vector of unknown regression coefficients and the generalized least squares estimator of $\boldsymbol{\beta}=(F^T\boldsymbol{R}^{-1}F)^{-1}F^T\boldsymbol{R}^{-1}Y^n$.

The Product Power Exponential correlation is chosen as the correlation function for prediction:

$$R\left(h|\xi\right) = \prod_{i=1}^{d}\exp\left[-\theta_i|h_i|^{p_i}\right] \quad (5)$$

Where $\xi=(\theta,p)=(\theta_1,\ldots,\theta_d,p_1,\ldots,p_d)$ with $\theta_i\geq0$ and $0<p_i\leq2$, the ξ estimator is the maximum likelihood estimate (MLE).

In order to confirm the reliability of RSM reproducing CMAQ simulations, the above prediction method is validated through "leave-one-out cross validation" (LOOCV), out of sample validation and 2-D isopleths validation. The definition of LOOCV is to use a single observation from the original sample as the validation data, and the remaining observations as the training data to build prediction RSM. Out of sample validation

ACPD
10, 29809–29851, 2010

needs additional CMAQ cases which are not included in training samples, then RSM predictions are compared with those extra CMAQ simulations. Validation of 2-D isopleths compares the prediction results of 2-D isopleths with that of multi-dimension RSM system, which is used to evaluate the stability of RSM system with higher dimensions.

Point-to-point data are compared through correlation analysis and error analysis. The correlation coefficient (R) and Mean Normalized Error (MNE) are calculated through following equations:

$$R = \sqrt{\frac{\left[\sum_{i=1}^{N}\left(M_i-\bar{M}\right)\left(O_i-\bar{O}\right)\right]^2}{\sum_{i=1}^{N}\left(M_i-\bar{M}\right)^2\sum_{i=1}^{N}\left(O_i-\bar{O}\right)^2}} \quad (6)$$

$$\mathrm{MNE} = \frac{1}{N}\sum_{i=1}^{N}\frac{|M_i-O_i|}{O_i} \quad (7)$$

Where M_i and O_i are the RSM predicted and CMAQ simulated value of the ith data in the series (temporal or spatial); and $\bar{M}$ and $\bar{O}$ are the average RSM predicted and CMAQ simulated value over the series.

3 Results and discussion

3.1 Development and validation of RSM-ozone system

The results of RSM modeling case LHS1_30 (as shown in Table 2) were used as "quasi-response" in preliminary experiments. The results of modeling case HSS6_200 (as shown in Table 2) were compared with that of LHS1_30 through leave-one-out cross validation, out-of-sample validation and 2-D isopleths validation. Sensitivity analysis was conducted to check the RSM prediction performance to the marginal level, sample numbers, and variable numbers.

ACPD
10, 29809–29851, 2010

3.1.1 Validation of RSM performance

Using the LOOCV method, the ozone levels simulated by CMAQ and predicted by RSM are compared for both case LHS1-30 (31 pairs of data) and case HSS6-200 (201 pairs of data), as shown in Fig. 4. Strong linear relationship (y=x) between CMAQ and RSM datasets are found in all areas for both cases, with square of R are larger than 0.99. For Beijing, Shanghai, Guangzhou and East China, the mean normalized errors (NE) of LHS1-30/HSS6-200 are respectively 0.2%/0.6%, 0.4%/0.6%, 0.9%/0.5%, and 0.3%/0.2%, and the maximum NEs are respectively 1.5%/4.1%, 2.7%/8.3%, 6.0%/5.5%, and 1.6%/1.8%. These results suggest that RSM prediction gives pretty good performance for all levels of ozone mixing ratio in both LHS1-30 and HSS6-200 cases.

Extra CMAQ simulations with certain NO_x and VOC emission ratios, as seen in Table 3, have been conducted to validate the RSM prediction. For Beijing, Shanghai, Guangzhou and East China, the mean NEs of LHS1-30/HSS6-200 are respectively 1.9%/1.2%, 0.7%/0.4%, 0.5%/0.5% and 0.5%/0.6%, and the maximum NEs of LHS1-30/HSS6-200 are respectively 3.9%/3.5%, 1.8%/2.0%, 1.8%/5.5% and 1.6%/1.8%. These results indicate that the RSM predictions are with good accuracy compared to CMAQ simulations, though relative larger biases occurred for low ozone mixing ratios.

The 2-D isopleths of Ozone responses to the emission changes of total NO_x and total VOC in HSS6-200 are given in Fig. 5a. From Fig. 5a, we can see the strong non-linear response of ozone to precursors' emissions in the three megacities. RSM is able to reveal such non-linear relationship between the responses of ozone concentrations to the changes precursors' emissions in an efficient and reliant way. The 2-D isopleths of NE, as shown in Fig. 5b, represents the differences between LHS1-30 and HSS6-200. The errors are below 1%. When NO_x emissions ratios are below 0.4 (60% of NO_x emissions reduced), larger NEs (2~15%) are found because of the marginal effects. Besides, the NO_x/VOC emission ratios corresponding to the inflection points are consistent in both LHS1-30 and HSS6-200. That confirms the stability of RSM with high dimensions (HSS6-200).

ACPD
10, 29809–29851, 2010

3.1.2 Sensitivity of RSM predictions to key parameters

As we discussed in Sect. 2.2, the optimized marginal level (n) is determined through computational experiments with "quasi-response" built in Sect. 2.3. Test samples are defined as all NO_x and VOC changes from 0.0 to 2.0 stepped by 0.1, respectively, total 441 pairs in all. Sensitivities of prediction performance to the marginal level are shown in Fig. 6. Six variables including 4 NO_x sources and 2 VOC sources are involved, sampled by two methods as LHS and HSS. In quasi-HSS-4vs2 (4 NO_x with 2 VOC sources, 100~160 samples), obvious improvement of prediction performance is found after marginal processing. Similar improvement is found in quasi-LHS-4vs2 (4 NO_x with 2 VOC sources, 160 samples), with level 3~4 marginal processing. The MNEs are reduced by 50%, from 8% to 3%.

In order to explore the sensitivity of prediction performance to numbers of samples and variables, we conduct a series of computational experiments with different variable and sample numbers using both LHS and HSS with marginal processing, as seen in Fig. 7. To obtain good prediction performance with MNE<1% and R>0.99, cases with few variable numbers such as 2(1 vs. 1) and 4(2 vs. 2) need small number of training samples (<30 for 2(1 vs. 1) and <60 for 4(2 vs. 2)). Errors increase along with the increase of variables. When the variable numbers are 6(4 vs. 2) and the sample number are over 150, the MNEs are still within acceptable range (<2%) and correlation coefficient (R) is over 0.99. However, when variable numbers are 8(6 vs. 2) and 10(8 vs. 2), MNEs are increased to 5% and 7% and correlation coefficient are decreased to 0.8 and 0.5, respectively. Increasing of sample numbers can not reduce the errors caused by the increase of variables, since the sample space is sharply enlarged with the increase of dimensions. That indicates there is a risk of statistics failure. Number of variables is the most crucial parameter that should be determined through computational experiments before one RSM case is established.

ACPD
10, 29809–29851, 2010

3.2 Application of ozone RSM in Beijing, Shanghai and Guangzhou

3.2.1 Identification of ozone chemistry

In the isopleths of ozone response to changes of precursor emissions predicted by RSM, the NO_x emission ratio at the peak ozone concentrations under baseline VOC emissions is defined as peak ratio, or ridge line ratio. When peak ratio is lower than current NO_x emission ratio (baseline emission ratio=1), the control of NO_x emissions may not effectively reduce ozone levels. When peak ratio is higher than current NO_x emission ratio, the control of NO_x emissions will effectively reduce ozone levels. Use of peak ratio as an index will not only help to identify the status of ozone response regime, but also indicate how much NO_x emission reduction may be needed to avoid the potential negative impacts on ozone reduction. We also compare the spatial distributions of NO_y mixing ratio and ratio of H_2O_2/HNO_3 to that of peak ratio and evaluate their robustness.

Due to the spatial variations of precursor concentrations, the ozone response varies in different locations (Xu et al., 2008). The spatial distributions of ozone concentrations, NO_y concentrations, H_2O_2/HNO_3, and peak ratios over three selected urban areas are shown in Fig. 8. The areas with peak ratio values less than 1 are mainly located in the city center in Beijing, Shanghai, Guangzhou, as well as Tianjin (in south of Beijing) and Hong Kong, due to the high density of NO_2 resulted from local emission sources. The spatial distributions of NO_y mixing ratio are consistent in all 3 regions, with the transition value around 15. In Beijing, similar results are given by the ratio of H_2O_2/HNO_3, with the transition value around 0.5. The results suggest that indicator of NO_y is more robust than the ratio of H_2O_2/HNO_3, adjusted transition value of H_2O_2/HNO_3 is needed for different locations, which is consistent with the results given by Zhang et al. (2009b). Also Peak Ratio is as good as NO_y, but peak ratio further serves an indicator for the degree of NO_x emissions needed to be reduced to become NO_x-limited from VOC-limited, which can be very important for designing urban ozone control strategy.

ACPD
10, 29809–29851, 2010

High ozone concentration usually appears in downwind rural areas such as the north of Beijing and Guangdong, rather than the city centers. The peak ratio changes from 0.8 to 1.2 along with the distance from city center. Similarly, NO_y mixing ratio changes from 20 ppb to 5 ppb. These results indicate that NO_x control is beneficial to ozone reduction in the downwind areas which usually have higher ozone mixing ratios than urban areas.

The ozone response varies with vertical height as well. The vertical profiles of peak ratio values and ozone mixing ratios in 3 cities are shown in Fig. 9. The peak ratio is lower than 1 in the surface layer of 3 cities. Therefore it is hardly seen the benefit of 70% NO_x reduction on ozone pollution in surface layer. While above layer 3~6 (vertical height 72~674 m), the peak ratio values are higher than 1, which indicates the strong benefits of NO_x control on ozone reduction. We can see the ozone responses when NO_x emission is reduced 50%~70%. Although the controls of NO_x emissions may not provide reduction of urban local ozone levels, it can reduce the downwind transport of ozone, and thus the benefit for regional air quality can be significant.

Due to the variation of in-situ meteorological conditions, including temperature, humidity, sunlight radiation density, as well as wind speed and precipitation, the ozone chemistry varies significantly in temporal scale, as shown in Fig. 10. During the days when higher ozone (>70 ppb) occurs under favorable meteorological condition for photochemical production of ozone, the ozone response is mostly NO_x-limited, with peak ratio around 0.8~1.5. However, in the days with lower ozone mixing ratio (<30 ppb), usually the effects of NO_x controls are negative for ozone, with peak ratio lower than 0.5, mainly because negative photochemical production leads to due to NO titration of ozone under high NO_x emissions (NO_x-rich conditions). This indicates that the control of NO_x emissions will benefit ozone reduction during high photochemical pollution period.

ACPD
10, 29809–29851, 2010

3.2.2 Evaluation of impacts from individual source

Sensitivity analyses are conducted using ozone RSM case HSS6-200 to understand the non-linear impacts of different source changes on surface ozone concentrations. The control effects of each source are presented in Fig. 11. "Ozone response" is defined as ozone change ratio to emission control ratio. Ozone responses to the changes of anthropogenic NMVOC (up to 100% control) are positive under baseline emissions of other sources, with a 15~18% ozone reduction in Beijing and Shanghai, and 25~30% ozone reduction in Guangzhou, as seen in Fig. 11a. The benefit for ozone reduction from both local and regional VOC emission control is always recognizable. But the VOC control benefit is decreasing with the strengthening of NO_x control level, as seen in Fig. 11b. Therefore, VOC control can be a more effective choice to reduce ozone if NO_x emissions stay at the same level.

The ozone is more sensitive to NO_x control under higher control level, compared to VOC emission control, as seen in Fig. 11b. Though NO_x controls usually benefit to ozone reduction in high ozone episodes as we discussed in last section, different NO_x sources affect ozone through different mechanisms. Regional NO_x sources are strong contributors to ozone concentration (10~20% ozone sensitivity in three cities), while local NO_x emission sources are negative contributor until more stringent control ratio reached (respectively 60%, 90% and 80% control in Beijing, Shanghai and Guangzhou by recalculating of combined control effects of two local NO_x emission sources). The reason is that the control of regional NO_x could significantly reduce the imported ozone (West et al., 2009), but the control of local NO_x has negative effects under VOC-limited regime. These results suggest that local controls can hardly solve regional air quality problem, for example, local NO_x emission control will increase local ozone mixing ratio. Synchronic control on VOC and regional emissions must be taken into account.

The non-linear relationship of ozone response to precursor emissions is obvious, as shown in Fig. 11. With the increase of emission reductions, ozone concentration is more sensitive to precursor emissions, shown as the grey line in Fig. 11a. These

ACPD
10, 29809–29851, 2010

results suggest that the effectiveness of NO_x emission control is strengthened with stricter control efforts. In addition, the interactions among different sources are obvious, as shown the red line in Fig. 11a. It's obvious that red lines in Fig. 11a (represent synchronic control of all emission sources) are above grey lines (represent sum of separate control on each source) when over 30% emissions are reduced. That indicates the enhancement of future control effectiveness should be considered when assessing the impacts of initial emission control actions, especially for NO_x emission control. One example is the control of NO_x from power plants. Although the direct benefit on surface ozone reduction from the control of NO_x from power plants is small, it considerably enhances the ozone reduction effects (see Fig. 11c). The effectiveness of control NO_x in other sources is enhanced by 1~2 times. Besides, the minimum emission control ratios to avoid the negative impacts of local NO_x control will be reduced from 60% to 40% in Beijing, from 100% to 50% in Shanghai, from 80% to 60% in Guangzhou.

Responses of ozone burdens to precursor emissions over the PBL (defined as layer 1~10, up to 3000 m) are shown in Fig. 11d. Compared to the responses of surface concentration (as shown in Fig. 11a), sensitivities of ozone burdens to VOC are smaller in all cities, mainly because of the changes of ozone chemistry in vertical profile. The negative impacts from the NO_x emission control of local area sources become weaker. However, the negative impacts from the NO_x emission control of power plants are even enlarged in Shanghai, which is because of the changes of ozone responses in different vertical height, as shown in Fig. 12. Sensitivity of ozone to NO_x emission in area sources decreases in upper layers but that to power plant NO_x emissions are even increasing over the PBL. Sensitivity of ozone to VOC emission decreases from Layer 1 to 12. Dominant sources in upper layers (above Layer 10) are regional NO_x emissions. The transitions of local NO_x impacts from low layers to upper layers are obvious in three cities, and the negative impacts in lower layers are weakened and positive impacts in upper layers (which contributes to regional air quality) are enhanced when strengthening control efforts. Similarly, the discrepancy between red line (represent synchronic control of all sources) and grey line (represent sum of separate control of each source)

ACPD
10, 29809–29851, 2010

indicates the obvious interactions among different sources, especially in Beijing and Shanghai.

3.2.3 Suggestion on control policies to achieve air quality standards

During the simulation period (July 2005), high ozone episodes that violate the National Ambient Air Quality Standards for ozone have been found in three cities, as seen in Fig. 13a. Besides, the downwind rural area usually has higher O_3 mixing ratios than urban area as we discussed in Fig. 8. Analysis on the Beijing surface observed O_3 mixing ratios in seven monitoring sites also indicates O_3 mixing ratios in Dingling (a downwind rural site in Beijing) are on average 10% (up to 60%) higher than other urban sites during polluted period. To guarantee the air quality in both urban and rural area, we choose 80% of the National Ambient Air Quality Standard of China, Class II, which equals to the Class I standard (1-h maximum less than 160 $\mu g\, m^{-3}$, approximately 80 ppb) as our policy target.

In order to meet this target, several optional control strategies are designed according to the RSM results (HSS6-200 case), as shown in Table 4. In option 1, we assume only local NO_x emissions are controlled. The local NO_x emissions in Beijing, Shanghai and Guangzhou are reduced 90%, 95% and 85%, respectively. In option 2, in addition to the same control of local NO_x sources as that in option 1, the local VOC sources are also subject to control. Regional NO_x controls are considered in option 3 and option 4. In option 3, both local NO_x emissions in Beijing, Shanghai, Guangzhou, and that from regional power plants will be reduced 80%, 85% and 80%. In option 4, additional controls on regional NO_x emissions from other sources are considered. In option 5 and option 6, we assume all NO_x and VOC emission sources are going to be controlled. All emission sources will be reduced 65%, 75% and 70% respectively for Beijing, Shanghai and Guangzhou in option 5. Since power plant are relatively easier to be controled, in option 6 we assume NO_x emissions from power plants will be reduced 80% and emissions of other sources will be reduced 60% and 65% and 60% respectively for Beijing, Shanghai and Guangzhou.

ACPD
10, 29809–29851, 2010

Ozone responses under those control strategies are given by Fig. 13a. Obvious control effectiveness is shown during high ozone days, and ozone mixing ratios are reduced to <80 ppb. However, the negative impacts still exist during lower ozone days, especially for option 1, 3 and 4 which only controlled NO_x emissions. In order to avoid control risk of ozone enhancement by NO_x controls under VOC-limited regime, VOC emissions should be synchronically reduced, as in option 5 and 6. The control effectiveness is noticeable over the region. The comparison of monthly averaged 1-h maximal ozone concentration between before-controlled (Fig. 13b) and after option 6-controlled (Fig. 13c) indicates the regional air qualities surrounding three cities get improved significantly.

The RSM can be applied to design the optimal (e.g., least-cost) control policy (Wang et al., 2001; Fu et al., 2006). When available NO_x/VOC control technologies are applied, the cumulative control cost functions can be estimated for each emission source. The quantitative relationship between ozone concentration and emission control cost can be determined through RSM. With certain environmental target (i.e., attainment of national ambient air quality standard), the optimized control ratio for each emission source can be calculated according to the minimal cost of the emission reduction.

Due to the atypical meteorological conditions as well as the uncertainties from simulations and predictions (rare public-opened observation data), those strategies are restricted in this case study. In addition, the potential growth of activities (e.g. energy consumption and vehicle population) is a big challenge for air quality which requires both more sustainable energy policy and better-planned control strategy in the future.

4 Conclusions

A response surface model for ozone control analysis is successfully developed using CMAQ air quality model. Good performances of RSM prediction are under all levels of ozone mixing ratio in both LHS1_30 and HSS6_200. NEs are within 10% and MNEs are within 1% during leave-one-out cross validation and out-of-sample validation. The

ACPD
10, 29809–29851, 2010

stability of RSM with high dimensions (HSS6_200) has been confirmed through 2-D isopleths validation. Through computational experiments, key parameters of ozone RSM development have been tested and determined. The maximum number for variables involving in statistical interpolation has better performance if not exceeding 8. Marginal processing applied in sampling (e.g., improving the boundary conditions) is recommended to improve the prediction performance, with MNEs reduced by 50%. However, the optimal number varies in different RSM designs (e.g., different control variables, or target pollutants). This paper only uses an efficient way (i.e., the preliminary experiment) to understand the prerequisite of a successful RSM experiment in the statistical aspect. The crucial parameters (i.e., variable number and run number) need to be carefully considered when using such a statistical method.

Peak ratio appears to be a useful index to understand the ozone formation in responding to the control of NO_x and VOC emissions. Spatial (both horizontal and vertical) and temporal variations must be considered when evaluating the emission control effects. In terms of horizontal distribution, NO_x control is usually beneficial for the downwind areas which usually have higher ozone concentrations than urban centers. The control of NO_x emission gives considerable benefits in upper layers (over 72~674 m) which can reduce the downwind transport of ozone. In the analysis of diurnal variations, the control of NO_x emissions is likely to be more effective than VOC emissions control during heavily polluted episode. Besides, the comparisons against the indicators of NO_y component and the ratio of H_2O_2/HNO_3 show that the peak ratio is a robust index as good as NO_y but can provide further important indication for the degree to NO_x emissions control needed to transition from VOC-limited to NO_x-limited regime for ozone control over the NO_x-rich urban areas.

Different emission sources affect ozone through different mechanisms. Ozone responses to VOC emission changes are always positive under baseline emissions of other sources. However, the effects of VOC emissions control significantly decrease with strengthening NO_x emissions control. Therefore, the control of NO_x emissions must be considered jointly with the VOC control to reduce urban local ozone. Regional

ACPD
10, 29809–29851, 2010

NO_x sources are important contributors to ozone concentration (10~20% ozone sensitivity in Beijing, Shanghai and Guangzhou), while local NO_x emission sources are negative contributors at surface because of the NO nitration of ozone under NO_x-rich urban areas. However, in the upper layers, sensitivities of ozone response to VOC are lower and the negative impacts from the local NO_x in urban areas become weaker compared to the responses of surface concentration. Local controls can not alone resolve the regional ozone issue, and thus synchronized control of VOC and NO_x emissions must be taken into consideration.

Strong non-linear relationship is obvious for ozone response to NO_x emissions. The effectiveness of NO_x emission control increases with strengthening control efforts. Therefore the enhancement of future control effectiveness must be considered when assessing the impacts of baseline emission control actions. Comprehensive control policy on multi-sources at both local and regional level is necessary to mitigate ozone problem in China.

Several control strategies are designed to meet this national ozone standard. Effectiveness of NO_x and VOC controls is obvious during high ozone days, and ozone levels can be reduced down to 80 ppb ozone standard. One of the cost-effective strategies is to reduce 80% of NO_x emissions from power plants and reduce 60% and 65% and 60% of emissions from other sources in Beijing, Shanghai and Guangzhou, respectively.

Acknowledgements. The study was financially supported by National High Technology Research and Development Program of China (2006AA06A309), Natural Science Foundation of China (20921140095), and the US EPA. The authors thank to Thomas J. Santner and Gang Han at Ohio State University for their helps on MperK program; Satoru Chatani from Toyota Central R&D Labs and Litao Wang, Qiang Zhang, Dan Chen at Tsinghua University for helping with emission processing.

ACPD
10, 29809–29851, 2010

References

Amann, M., Bertok, I., Borken, J., Chambers, A., Cofala, J., Dentener, F., Heyes, C., Hoglund, L., Klimont, Z., Purohit, P., Rafaj, P., Schöpp, W., Toth, G., Wagner F., and Winiwarter, W.: A tool to combat air pollution and climate change simultaneously. Methodology report, International Institute for Applied Systems Analysis (IIASA), Laxenburg, Austria, 2008.

Binkowski, F. S. and Roselle, S. J.: Models-3 Community Multiscale Air Quality (CMAQ) model aerosol component, 1. Model description, J. Geophys. Res., 108, 4183, doi:10.1029/2001JD001409, 2003.

Box, G. E. P. and Draper N.: Response Surfaces, Mixtures, and Ridge Analyses, Second Edition of Empirical Model-Building and Response Surfaces, 1987, Wiley, 2007.

Byun, D. W. and Schere, L. K.: Review of the governing equations,computational algorithms and other components of the models-3 Community Multiscale Air Quality (CMAQ) modeling system, Appl. Mech. Rev., 59(2), 51–77, 2006.

Cohan, D. S., Hakami, A., Hu, Y. T., and Russell, A. G.: Nonlinear response of ozone to emissions: source apportionment and sensitivity analysis, Environ. Sci. Technol., 39, 6739–6748, 2005.

Cohan, D. S., Tian, D., Hu, Y. T., and Russell, A. G.: Control strategy optimization for attainment and exposure mitigation: case study for ozone in Macon, Georgia, Environ. Manage., 38, 451–462, 2006.

Cohan, D. S., Boylan, J. W., Marmur, A., and Khan, M. N.: An integrated framework for multipollutant air quality management and its application in Georgia, Environ. Manage., 40, 545–554, 2007.

Dunker, A. M., Yarwood, G., Ortmann, J. P., and Wilson, G. M.: Comparison of source apportionment and source sensitivity of ozone in a three-dimensional air quality model, Environ. Sci. Technol., 36, 2953–2964, 2002.

ENVIRON: User's guide to the Comprehensive Air Quality Model with Extensions (CAMx), ENVIRON International Corporation, Novato, CA, 2002.

Fu, J. S., Brill Jr., E. D., and Ranjithan, S. R.: Conjunctive use of models to design cost-effective ozone control strategies, J. Air Waste Manage., 56, 800–809, 2006.

Hakami, A. Odman, M. T., and Russell, A. G.: High-order, direct sensitivity analysis of multidimensional air quality models, Environ. Sci. Technol., 37, 2442–2452, 2003.

ACPD
10, 29809–29851, 2010

Hammersley, J.: Monte Carlo methods for solving multivariable problems, Proceedings of the New York Academy of Science, 86, 844–874, 1960.
Heyes, C., Schopp, W., Amann, M., Bertok, I., Cofala, J., Gyarfas, F., Kilmont, Z., Makowski, M., and Shibayev, S.: A Model for Optimizing Strategies for Controlling Ground-Level Ozone in Europe, Interim Report IR-97-002/January, International Institute for Applied Systems Analysis, 1997, available at: http://www.iiasa.ac.at/Admin/PUB/Documents/IR-97-002.pdf, last access: November 2010.
Iman, R. L., Davenport, J. M., and Zeigler, D. K.: Latin Hypercube Sampling (Program User's Guide), Technical Report SAND79-1473, Sandia National Laboratories, Albuquerque, NM, 1980.
Jang, J. C., Jeffries, H. E., and Tonnesen, S.: Sensitivity of ozone to model grid resolution-II. Detailed process analysis for ozone chemistry, Atmos. Environ., 29, 3101–3114, 1995.
Klimont, Z., Cofala, J., Xing, J., Wei, W., Zhang, C., Wang, S., Kejun, J., Bhandari, P., Mathur, R., Purohit, P., Rafaj, P., Chambers, A., and Amann, M.: Projections of SO_2, NO_x and carbonaceous aerosols emissions in Asia, Tellus B, 61, 602–617, 2009.
Lei, Y., He, K. B., Zhang, Q., and Liu, Z. Y.: Technology-based emission inventory of particulate matters (PM) from cement industry, Environ. Sci., 29, 2366–2371, 2008 (in Chinese).
Li, L., Chen, C. H., Huang C., Huang H. Y., Li Z. P., Fu, S. J., Jang J. C., and Streets, D. G.: Regional air pollution characteristics simulation of O_3 and PM_{10} over Yangtze River Delta Region, Environ. Sci., 29(1), 237–45, 2008 (in Chinese).
Liu, X. H., Zhang, Y., Xing, J., Zhang, Q., Streets, D. G., Jang, C. J., Wang, W. X., and Hao, J. M.: Understanding of regional air pollution over China using CMAQ – Part II. Process analysis and ozone sensitivity to precursor emissions, Atmos. Environ., 44, 3719–3727, 2010.
Milford, J. B., Russell, A. G., and McRae, G. J.: A new approach to photochemical pollution control: implications of spatial patterns in pollutant responses to reductions in nitrogen oxides and reactive organic gas emissions, Environ. Sci. Technol., 23, 1290–1301, 1989.
Ohara, T., Akimoto, H., Kurokawa, J., Horii, N., Yamaji, K., Yan, X., and Hayasaka, T.: An Asian emission inventory of anthropogenic emission sources for the period 1980–2020, Atmos. Chem. Phys., 7, 4419–4444, doi:10.5194/acp-7-4419-2007, 2007.
Ran, L., Zhao, C., Geng, F., Tie, X., Tang, X., Peng, L., Zhou, G., Yu, Q., Xu, J., and Guenther, A.: Ozone photochemical production in urban Shanghai, China: analysis based on ground level observations, J. Geophys. Res., 114, D15301, doi:10.1029/2008JD010752, 2009.

ACPD
10, 29809–29851, 2010

Santner, T. J., Williams, B. J., and Notz, W.: The Design and Analysis of Computer Experiments, Springer Verlag, New York, 2003.
Seinfeld, J. H. and Pandis, S. N.: Atmospheric Chemistry and Physics: From Air Pollution to Climate Change, John Wiley and Sons, Inc., New York, 241 pp., 2006.
Shao, M., Tang, X., Zhang, Y., and Li, W.: City clusters in China: air and surface water pollution, Front. Ecol. Environ., 4, 353–361, 2006.
Shao, M., Zhang, YH, Zeng, L.-M., Tang, X.-Y., Zhang, J., Zhong, L.-J., and Wang, B.-G.: Ground-level ozone in the Pearl River Delta and the roles of VOC and NO_x in its production, J. Environ. Manage., 90, 512–518, 2009.
Shih, J. S., Russell, A. G., and McRae, G. J.: An optimization model for photochemical air pollution control, Eur. J. Oper. Res., 106, 1–14, 1998.
Sillman, S.: The use of NO_y, H_2O_2, and HNO_3 as indicators for ozone-NO_x-hydrocarbon sensitivity in urban locations. J. Geophys. Res., 100(D7), 4175–4188. 1995.
Streets, D. G., Fu, J. S., Jang, C. J., Hao, J. M., He, K. B., Tang, X. Y., Zhang, Y. H., Wang, Z. F., Li, Z. P., Zhang, Q., Wang, L. T., Wang, B. Y., and Yu, C.: Air quality during the 2008 Beijing Olympic Games, Atmos. Environ., 41, 480–492, 2007.
Tang, G., Li, X., Wang, Y., Xin, J., and Ren, X.: Surface ozone trend details and interpretations in Beijing, 2001–2006, Atmos. Chem. Phys., 9, 8813–8823, doi:10.5194/acp-9-8813-2009, 2009.
Tie, X.-X., Geng, F.-H., Peng, L., Gao, W., and Zhao, C.-S.: Measurement and modeling of O_3 variability in Shanghai, China: application of the WRF-Chem model, Atmos. Environ., 43, 4289–4302, 2009.
Tonnesen, G. S. and Dennis, R. L.: Analysis of radical propagation efficiency to assess ozone sensitivity to hydrocarbons and NO_x 1. Local indicators of instantaneous odd oxygen production sensitivity, J. Geophys. Res., 105(D7), 9213–9225, 2000.
US Environmental Protection Agency: Technical Support Document for the Proposed Mobile Source Air Toxics Rule: Ozone Modeling, Office of Air Quality Planning and Standards, Research Triangle Park, NC, 2006a.
US Environmental Protection Agency: Technical Support Document for the Proposed PM NAAQS Rule: Response Surface Modeling, Office of Air Quality Planning and Standards, Research Triangle Park, NC, 2006b.
Wang, L. H. and Milford, J. B.: Reliability of optimal control strategies for photochemical air pollution., Environ. Sci. Technol., 35, 1173–1180, 2001.

ACPD
10, 29809–29851, 2010

Wang, H., Zhou, L., and Tang, X.: Ozone concentrations in rural regions of the Yangtze Delta in China, J. Atmos. Chem., 54, 255–265, 2006a.
Wang, T., Ding, A. J., Gao, J., and Wu, W.-S.: Strong ozone production in urban plumes from Beijing, China, Geophys. Res. Lett., 33, L21806, doi:10.1029/2006GL027689, 2006b.
Wang, Z., Li, J., Wang, X., Pochanart, P., and Akimoto, H.: Modeling of regional high ozone episode observed at two mountain sites (Mt. Tai and Huang) in East China, J. Atmos. Chem., 55, 253–272, 2006c.
Wang, L. T., Hao, J. M., He, K. B., Wang, S. X., Li, J. H., Zhang, Q., Streets, D. G., Fu, J. S., Jang, C. J., Takekawa, H., and Chatani, S.: A modeling study of coarse particulate matter pollution in Beijing: regional source contributions and control implications for the 2008 Summer Olympics, J. Air Waste Manage., 58, 1057–1069, 2008.
Wang, X. S., Li, J.-L., Zhang, Y. H., Xie, S. D., and Tang X. Y.: Ozone source attribution during a severe photochemical smog episode in Beijing, China, Sci. China, 39-6, 548–559, 2009.
Wang, L. T., Jang, C., Zhang, Y., Wang, K., Zhang, Q., Streets, D., Fu, J., Lei, Y., Schreifels, J., He, K. B., Hao, J. M., Lam, Y. F., Lin, J., Meskhidze, N., Voorchees, S., Evarts, D., and Phillips, S.: Assessment of air quality benefits from national air pollution control policies in China. Part I: Background, emission scenarios and evaluation of meteorological predictions, Atmos. Environ., 44, 3442–3448, 2010a.
Wang, S. X., Zhao, M., Xing, J., Wu, Y., Zhou, Y., Lei, Y., He, K. B., Fu, L. X., and Hao, J. M.: Quantifying the air pollutants emission reduction during the 2008 Olympic Games in Beijing, Environ. Sci. Technol., 44(7), 2490–2496, doi:10.1021/es9028167, 2010b.
Wei, W., Wang, S. X., Chatani, S., Klimont, Z., Cofala, J., and Hao, J. M.: Emission and speciation of non-methane volatile organic compounds from anthropogenic sources in China, Atmos. Environ., 42(20), 4976–4988, 2008.
West, J. J., Naik, V., Horowitz, L. W., and Fiore, A. M.: Effect of regional precursor emission controls on long-range ozone transport – Part 1: Short-term changes in ozone air quality, Atmos. Chem. Phys., 9, 6077–6093, doi:10.5194/acp-9-6077-2009, 2009.
Xing, J., Wang, S. X., Chatani., S., Cofala, J., Klimont, Z., Amann, M., and Hao, J. M.: Validating anthropogenic emissions of China by satellite and surface observations, Atmos. Environ, in review, 2010.
Xu, J., Zhang, Y. H., Fu, J. S., Zheng, S. Q., and Wang, W.: Process analysis of typical summertime ozone episodes over the Beijing area, Sci. Total Environ., 399, 147–157, 2008.
Zhang, Y., Vijayaraghavan, K., and Seigneur, C.: Evaluation of three probing tech-

ACPD
10, 29809–29851, 2010

niques in a three-dimensional air quality model, J. Geophys. Res., 110, D02305, doi:10.1029/2004JD005248., 2005.
Zhang, Y. H., Huang, W., London, S. J., Song, G. X., Chen, G. H., Jiang, L. L., Zhao, N. Q., Chen, B.-H., and Kan, H.-D.: Ozone and daily mortality in Shanghai, China, Environ. Health Persp., 114, 1227–1232, 2006.
Zhang, Y. H., Su, H., Zhong, L. J. , Cheng, Y. F., Zeng, L. M., Wang, X. S., Xiang, Y. R., Wang, J. L., Gao, D. F., Shao, M., Fan, S. J., and Liu, S. C.: Regional ozone pollution and observation-based approach for analyzing ozone–precursor relationship during the PRIDE-PRD2004 campaign, Atmos. Environ., 42, 6203–6218, 2008.
Zhang, Q., Streets, D. G., Carmichael, G. R., He, K. B., Huo, H., Kannari, A., Klimont, Z., Park, I. S., Reddy, S., Fu, J. S., Chen, D., Duan, L., Lei, Y., Wang, L. T., and Yao, Z. L.: Asian emissions in 2006 for the NASA INTEX-B mission, Atmos. Chem. Phys., 9, 5131–5153, doi:10.5194/acp-9-5131-2009, 2009a.
Zhang, Y., Wen, X. Y., Wang, K., Vijayaraghavan, K., and Jacobson, M. Z.: Probing into regional O_3 and PM pollution in the US, Part II: An examination of formation mechanisms through a process analysis technique and sensitivity study, J. Geophys. Res., 114, D22305, doi:10.1029/2009JD011900, 2009b.
Zhao, Y., Wang, S. X., Duan, L., Lei, Y., Cao, P. F., and Hao, J. M.: Primary air pollutant emissions of coal-fired power plants in China: current status and future prediction, Atmos. Environ., 42, 8442–8452, 2008.
Zheng, J., Zhang L. J., Che, W. W, Zheng, Z. Y., and Yin, S. S.: A highly resolved temporal and spatial air pollutant emission inventory for the Pearl River Delta region, China and its uncertainty assessment, Atmos. Environ., 43, 5112–5122, 2009.

ACPD
10, 29809–29851, 2010

Table 1. Summary of National Emissions in China in 2005 (unit: kt/year).

	SO_2	NO_x	PM_{10}	$PM_{2.5}$	BC	OC	NH_3	VOC
Power Plants	15 826	6965	1851	1024	49	20	1	295
Industrial Combustion	7060	3272	2787	1828	314	146	5	–
Industrial Processes	2864	1824	6829	4368	297	251	173	5779
Cement	1321	1282	4829	3083	18	31	–	–
Iron	931	212	432	317	3	23	–	–
Domestic sources	2458	1335	5220	4656	749	2486	96	1586
Biofuel	529	559	4388	4251	623	2415	94	–
Transportation	387	4763	441	326	140	138	2	5601
Others	56	340	2110	2044	46	453	16 279	6054
Open Biomass Burning	56	340	2110	2044	46	453	14	5871
Livestock Farming	–	–	–	–	–	–	7161	–
Mineral Fertilizer Application	–	–	–	–	–	–	8354	–
National total emissions	28 651	18 499	19 237	14 245	1595	3494	16 556	19 406

ACPD
10, 29809–29851, 2010

Table 2. Sample methods and key parameters used for ozone response surface establishment.

RSM case	Variable number	Sample method	Sample number
LHS1-30	Total-NO_x and Total-VOC	Latin Hypercube Sampling without margin process	30
HSS6-200	Local NO_x in Power plants; Local NO_x in Area sources; Local VOC; Regional NO_x in Power plants; Regional NO_x in Area sources; Regional VOC;	Hammersley quasi-random Sequence Sample with margin level as 6	200

ACPD
10, 29809–29851, 2010

Table 3. Normalized errors of RSM predicted daily 1-h maximal ozone mixing ratio compared to that simulated by CMAQ through out-of-sample validation, %.

	Emission Ratio		Beijing		Shanghai		Guangzhou		East China	
No	NO_x	VOC	LHS1-30	HSS6-200	LHS1-30	HSS6-200	LHS1-30	HSS6-200	LHS1-30	HSS6-200
1	0.1	1	2.0	−2.5	1.8	−3.6	−1.5	−0.7	−0.9	−0.2
2	0.3	1	3.2	−1.4	0.5	−2.0	−0.3	−0.2	−1.6	0.1
3	0.5	1	2.8	1.3	−1.0	0.0	0.1	−0.1	−1.5	0.0
4	0.7	1	2.3	1.6	−0.9	1.1	−0.2	0.5	−1.6	−0.8
5	1.5	1	−1.3	−0.4	0.5	−0.5	0.3	0.4	−0.3	−0.2
6	1.9	1	−3.9	−0.2	−1.0	−0.6	−0.1	−0.3	−0.2	0.0
7	1	0.1	0.3	−2.0	0.9	−1.0	−0.6	0.3	−0.1	−1.2
8	1	0.3	0.7	−1.4	0.8	−0.8	0.0	0.5	0.0	−1.4
9	1	0.5	0.9	−0.9	0.5	−0.9	0.4	0.5	−0.3	−1.5
10	1	0.7	1.0	−0.6	0.1	−1.1	0.3	0.0	−0.3	−1.6
11	1	1.5	1.5	0.0	−0.7	−0.7	0.0	0.2	0.0	−1.4
12	1	1.9	1.7	0.3	−1.3	−0.5	−0.1	0.7	−0.1	−1.1
13	0.1	0.1	1.1	−3.5	0.5	−1.7	−2.0	−1.8	−0.7	−0.6
14	0.3	0.3	3.5	−1.9	1.2	−1.6	−0.5	−1.8	−0.1	−0.1
15	0.5	0.5	2.6	1.0	−0.4	0.6	−0.3	−1.0	0.1	−0.1
16	0.7	0.7	2.2	1.4	−0.1	1.2	−0.2	0.1	−0.1	−0.8
17	1.5	1.5	−0.5	−0.3	0.4	0.0	0.1	0.3	0.2	−0.2
18	1.9	1.9	−2.1	−0.3	−0.8	−0.3	−0.6	0.2	−1.0	0.0
Mean Normalized Error			1.9	1.2	0.7	0.4	0.5	0.5	0.5	0.6
Maximal Normalized Error			3.9	3.5	1.8	2.0	1.8	5.5	1.6	1.8

ACPD
10, 29809–29851, 2010

Table 4. Optional NO_x/VOC emission reduction ratios to meet the National Ambient Air Quality Standard in China for ozone (1-h maximal concentration, 160 μg/m^3).

	Local NO_x PP	Local NO_x Other	Local VOC	Regional NO_x PP	Regional NO_x Other	Regional VOC
Beijing						
Option 1	90%	90%				
Option 2	80%	80%	80%			
Option 3	80%	80%		80%		
Option 4	75%	75%		75%	75%	
Option 5	65%	65%	65%	65%	65%	65%
Option 6	80%	60%	60%	80%	60%	60%
Shanghai						
Option 1	95%	95%				
Option 2	95%	95%	95%			
Option 3	85%	85%		85%		
Option 4	80%	80%		80%	80%	
Option 5	75%	75%	75%	75%	75%	75%
Option 6	80%	65%	65%	80%	65%	65%
Guangzhou						
Option 1	85%	85%				
Option 2	85%	85%	85%			
Option 3	80%	80%		80%		
Option 4	75%	75%		75%	75%	
Option 5	70%	70%	70%	70%	70%	70%
Option 6	80%	60%	60%	80%	60%	60%

Note: Option 1 – local NO_x control only; Option 2 – local sources control only; Option 3 – power plants and local NO_x control only; Option 4 – NO_x control only; Option 5 – control of all sources; Option 6 – maximal control of power plant.

ACPD
10, 29809–29851, 2010

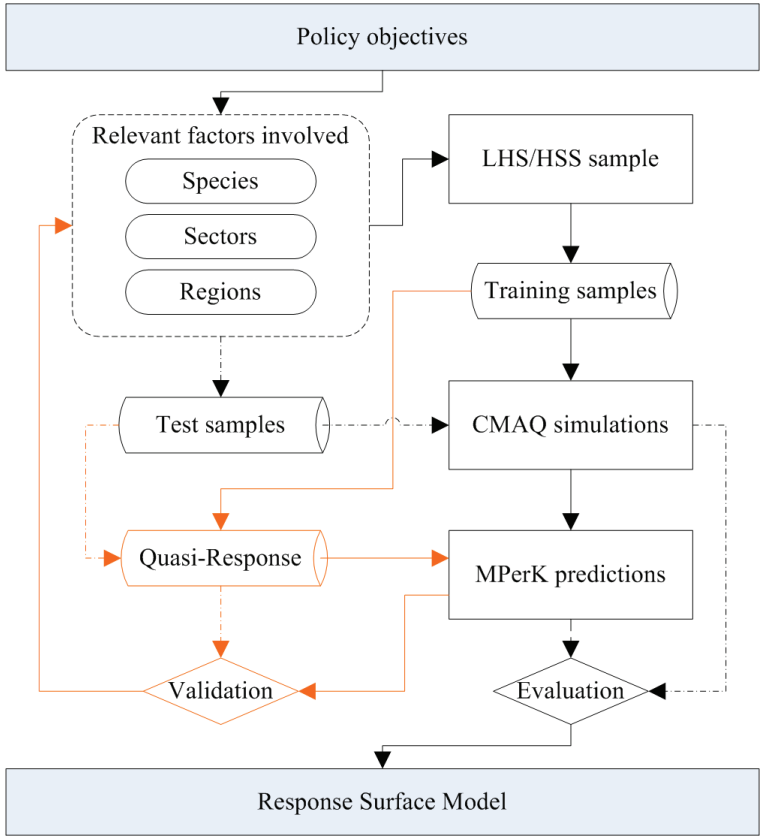

Fig. 1. Key steps in the development of response surface model (orange lines indicate the preliminary experiment to determine the crucial parameters used to establish RSM).

ACPD
10, 29809–29851, 2010

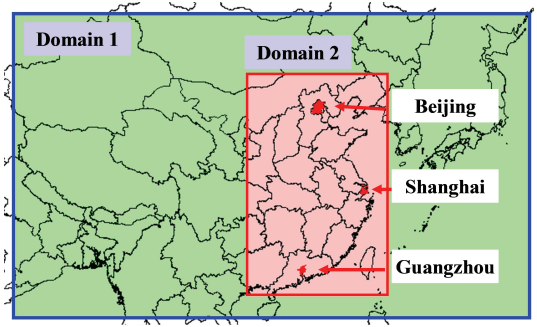

(a) CMAQ and RSM modeling domain

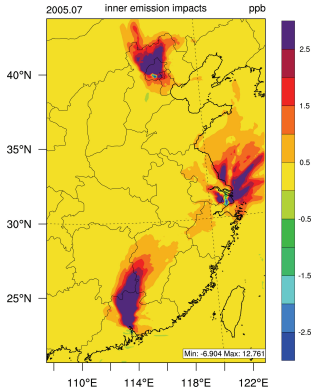

(b) interactions among three cities

Fig. 2. Map of the CMAQ/RSM modeling domain and interactions among three cities (monthly mean of 1-h daily ozone maxima in July 2005, unit: μg/m^3).

ACPD
10, 29809–29851, 2010

Nonlinear response of ozone to precursor emission changes in China

J. Xing et al.

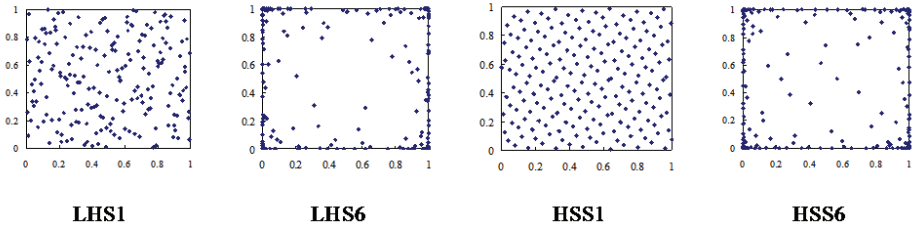

(a) Joint distribution of two individual variables (200 samples in [0~1])

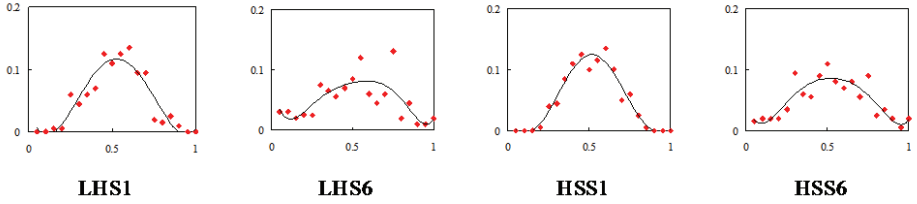

(b) Distribution density of sum 4 variables (200 samples in [0~1], red-point represents sample distribution density, dark-line is the fitting trend-line with 4th power)

Fig. 3. Margin processing conducted in sampling.

ACPD
10, 29809–29851, 2010

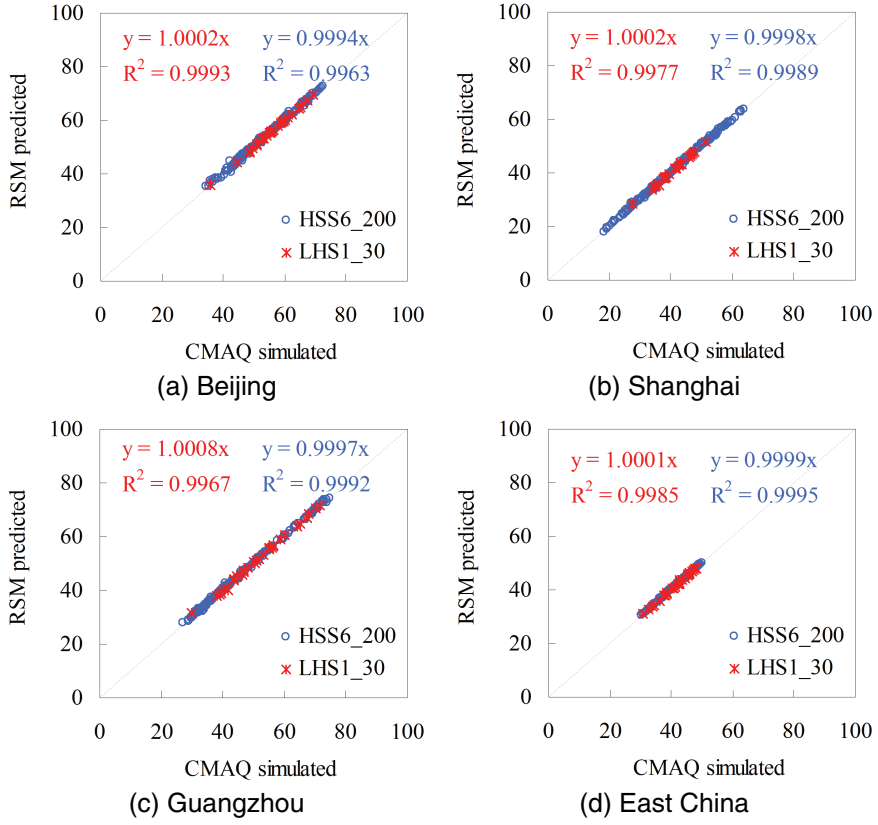

Fig. 4. Leave-one-out cross-validation of two RSM-ozone cases (monthly mean of daily 1-h maxima ozone, ppb).

ACPD
10, 29809–29851, 2010

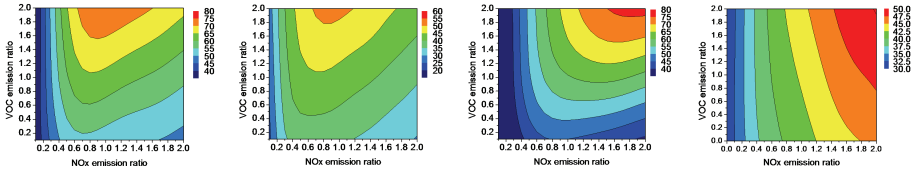

(a) 2-D Isopleths of Ozone (monthly mean of daily 1-h maxima, ppb)

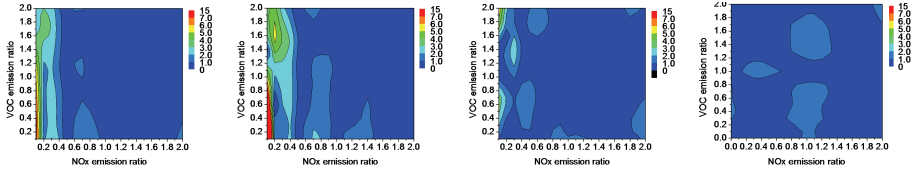

(b) Normalized error (equal absolute (HSS6-200 minus LHS1-30) divided by LHS1-30, %)

Fig. 5. 2-D isopleths validation of HSS6-200.

ACPD
10, 29809–29851, 2010

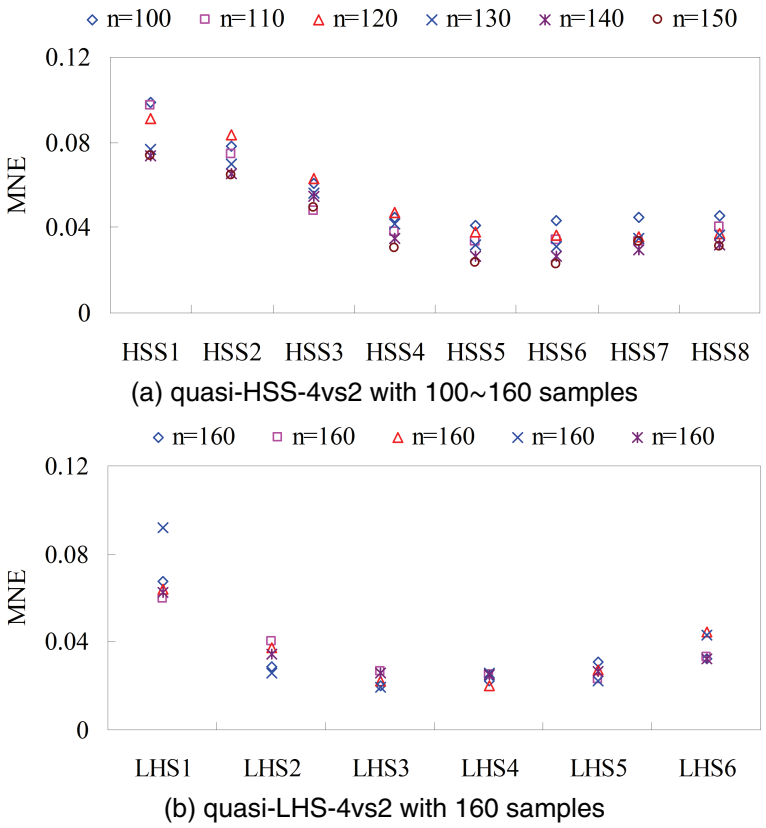

Fig. 6. Sensitivity of prediction performances to marginal level through computational experiments.

ACPD
10, 29809–29851, 2010

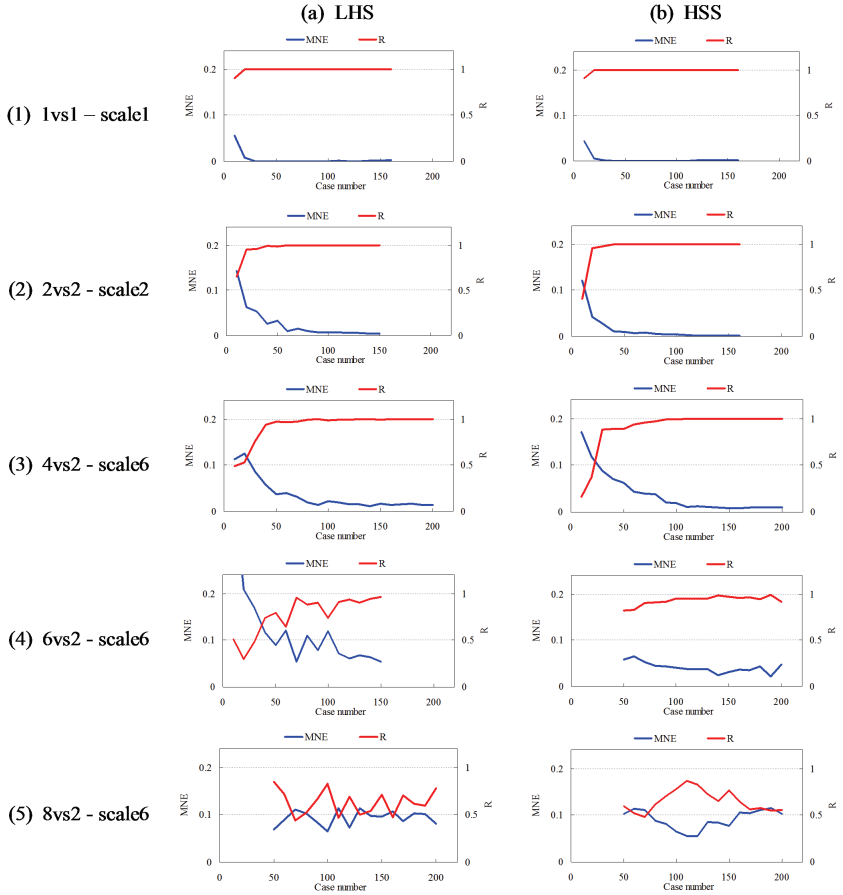

Fig. 7. Sensitivity of prediction performances to sample number and variable numbers through computational experiments.

ACPD
10, 29809–29851, 2010

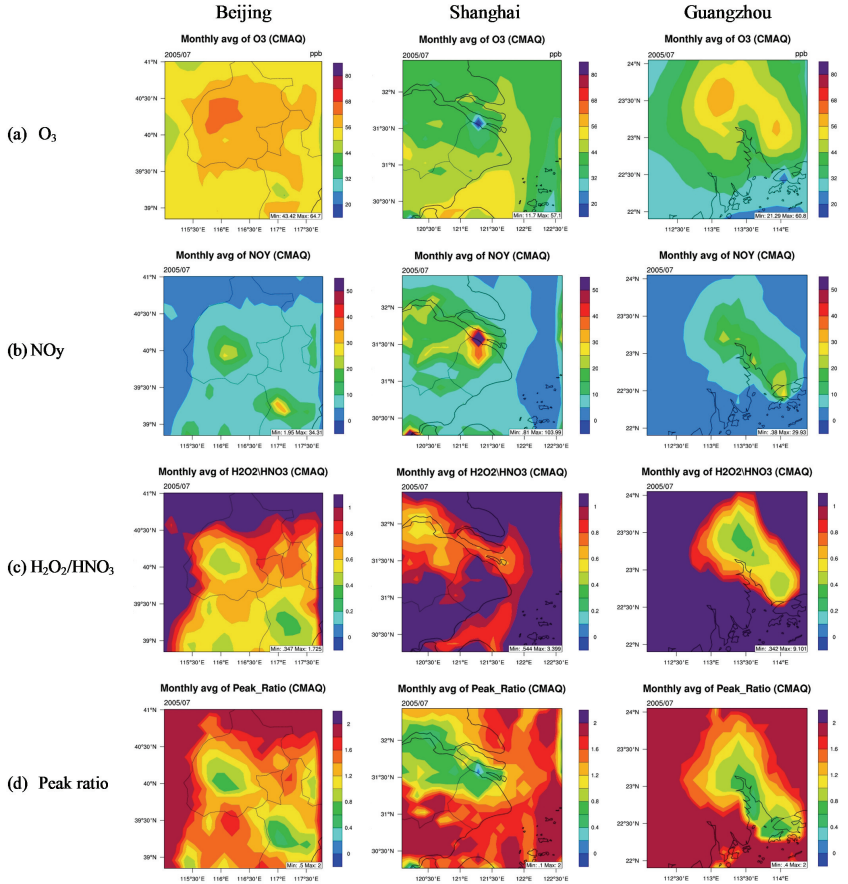

Fig. 8. Ozone chemistry variations in Beijing, Shanghai and Guangzhou (monthly mean of ozone mixing ratio during afternoon time, 12:00~17:00).

ACPD
10, 29809–29851, 2010

Nonlinear response of ozone to precursor emission changes in China

J. Xing et al.

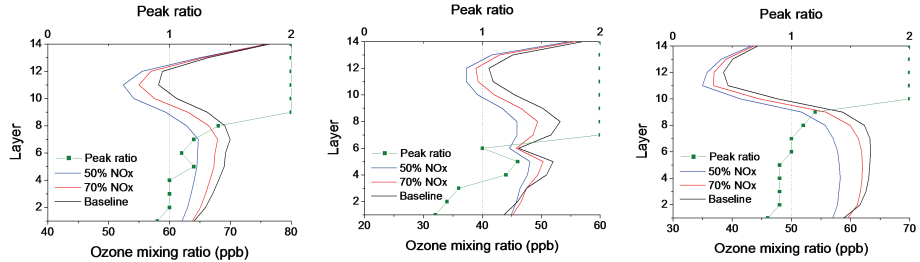

Fig. 9. Vertical profile of peak ratio and ozone mixing ratio in Beijing, Shanghai and Guangzhou (monthly mean during afternoon time, 12:00~17:00; The height of layers 1–14 above ground are 36, 72, 145, 294, 444, 674, 1070, 1568, 2093, 2940, 3991, 5807, 9057, 14 648 m, respectively).

ACPD
10, 29809–29851, 2010

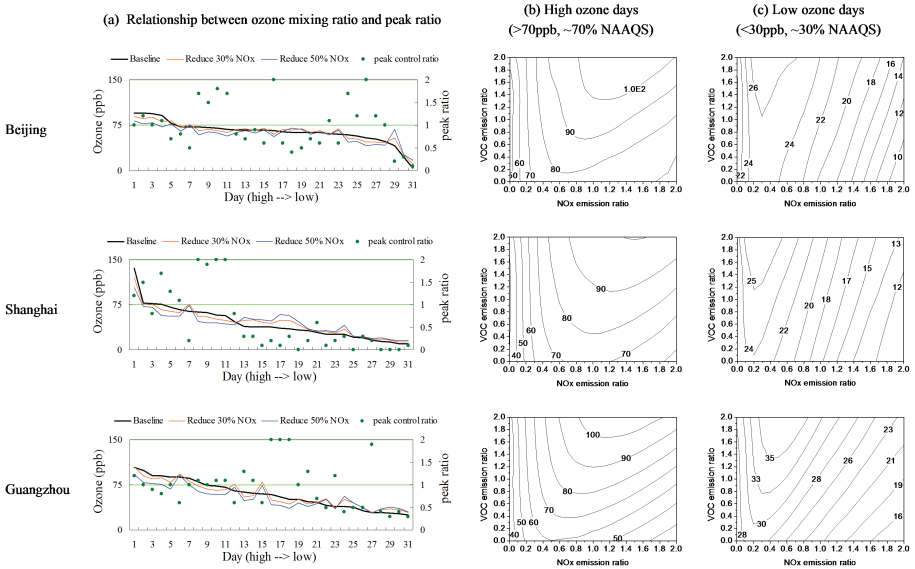

Fig. 10. Daily variation of ozone chemistry in 3 cities (daily-maxima, July 2005).

ACPD
10, 29809–29851, 2010

Nonlinear response of ozone to precursor emission changes in China

J. Xing et al.

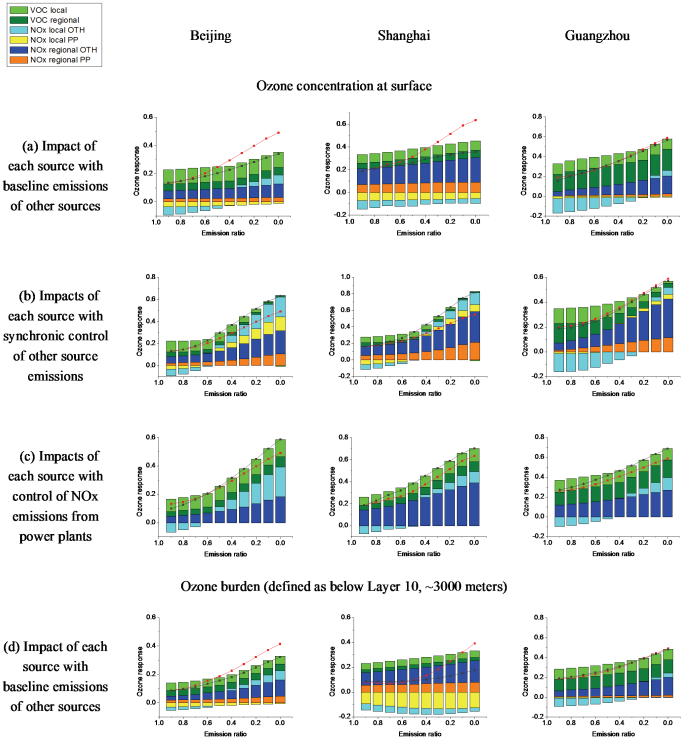

Fig. 11. Ozone response to the stepped control of individual source in 3 cites. (Ozone response=change of ozone/(1 – emission ratio); red solid lines indicate synchronic control of all sources; colored columns are ozone response to the changes of each source; grey solid lines indicate sum of separate control on each source; all values are averaged of 1-h maxima ozone in high ozone days in July 2005.)

ACPD
10, 29809–29851, 2010

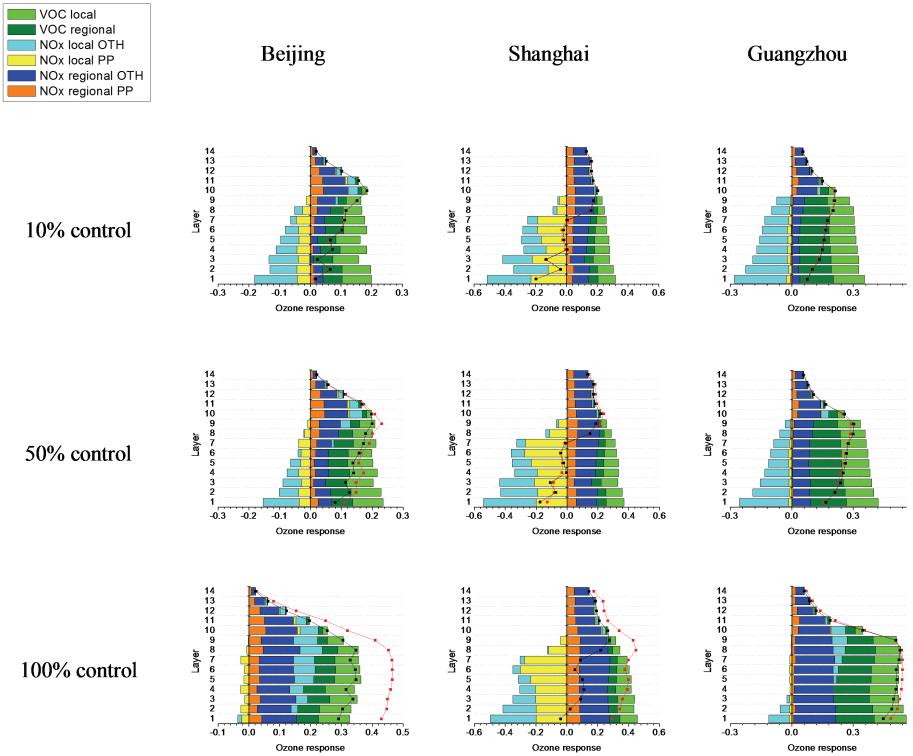

Fig. 12. Vertical profile Ozone response to the stepped control of individual source in 3 cites. (Ozone response=change of ozone/(1 – emission ratio); red solid lines indicate synchronic control on all sources; colored columns are ozone response to the changes of each source; grey solid lines indicate sum of separate control on each source; the height of layers 1–14 above ground are 36, 72, 145, 294, 444, 674, 1070, 1568, 2093, 2940, 3991, 5807, 9057, 14 648 m, respectively; all values are averaged of ozone during afternoon time, 12:00~17:00 in July 2005.)

ACPD
10, 29809–29851, 2010

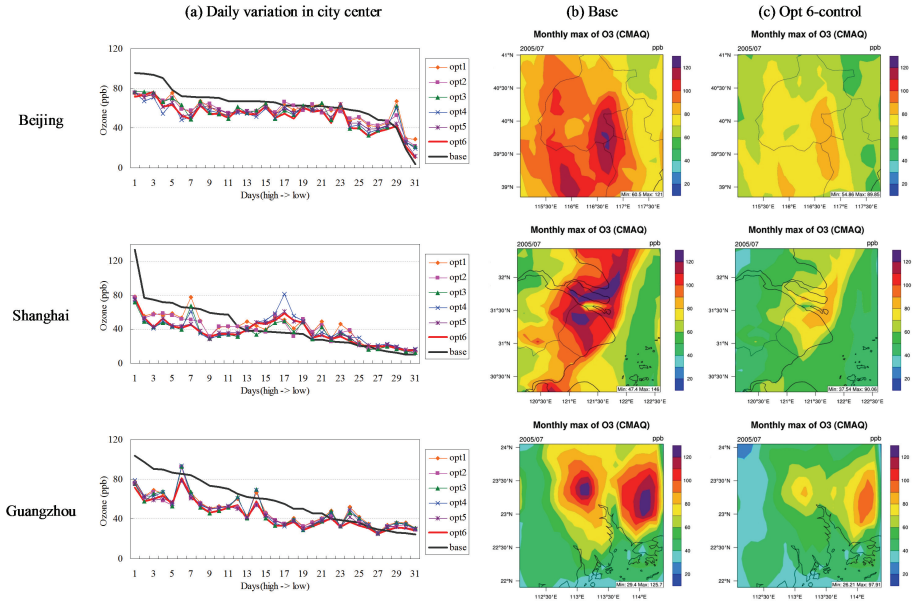

Fig. 13. Effectiveness of NO_x/VOC control strategies to achieve secondary national ozone standards in 3 cities (daily-maxima, July 2005).

ACPD
10, 29809–29851, 2010